SPANDIDOS
PUBLICATIONS

MicroRNA-103 modulates tumor progression by targeting KLF7 in non-small cell lung cancer

KE LI[1] and CONGHU YUAN[2]

[1]Department of Oncology, Jiangsu Cancer Hospital and Jiangsu Institute of Cancer Research and
The Affiliated Cancer Hospital of Nanjing Medical University, Nanjing, Jiangsu 210009; [2]Department of Anesthesiology,
The Third People's Hospital of Yancheng, Yancheng, Jiangsu 224000, P.R. China

Abstract. Numerous studies have identified that microRNAs (miRs) play a crucial role in the tumorigenesis of non-small cell lung cancer (NSCLC). However, to the best of our knowledge, the physiological function of miR-103 in NSCLC is not fully understood. Experiments in the present study revealed that miR-103 expression was increased in NSCLC cell lines. In addition, a series of methods, including MTT, colony formation, 5-ethynyl-2'-deoxyuridine, Transwell, wound healing, flow cytometric, reverse transcription-quantitative PCR and western blot assays, were performed, which revealed that overexpression of miR-103 enhanced cell growth, migration, invasion and epithelial-mesenchymal transition (EMT), and suppressed apoptosis of A549 and H1299 cells. Additionally, a dual-luciferase reporter assay indicated that miR-103 directly targets the 3'-untranslated region of Kruppel-like factor 7 (KLF7), and KLF7 expression was negatively regulated by miR-103 expression. Furthermore, the present findings demonstrated that miR-103 promoted EMT via regulating the Wnt/β-catenin signaling pathway in NSCLC. Collectively, the current results demonstrated that miR-103 serves a tumorigenesis role in NSCLC development by targeting KLF7, at least partly via the Wnt/β-catenin signaling pathway. Consequently, these findings indicated that miR-103/KLF7/Wnt/β-catenin may provide a novel insight into underlying biomarkers for improving the diagnosis and treatment of NSCLC.

Correspondence to: Dr Ke Li, Department of Oncology, Jiangsu Cancer Hospital and Jiangsu Institute of Cancer Research and The Affiliated Cancer Hospital of Nanjing Medical University, 42 Baiziting Road, Nanjing, Jiangsu 210009, P.R. China
E-mail: kelimdphd@163.com

Introduction

Lung cancer is the most frequent malignancy and is the leading cause of cancer-associated mortality worldwide, with an estimated 2.1 million newly diagnosed cases and 1.8 million deaths reported in 2018 (1,2). Non-small cell lung cancer (NSCLC) is a primary class of lung cancer and ~85% of lung cancer cases are classified as NSCLC (3,4). Although great advancements have made in the clinic, the prognosis of NSCLC remains poor and the 5 year survival rate of patients from Europe with NSCLC remained at <15% in 2016, which may be due to the limitations of early detection methods (5-7). Thus, numerous recent studies have focused on investigating the molecular mechanisms associated with NSCLC progression in order to identify novel treatment methods (8-10).

MicroRNAs (miRNAs or miRs) are small endogenous non-coding RNAs that are ~1,822 nucleotides in length (11). miRNAs exert important functions on human gene expression regulation via binding to the 3'-untranslated region (3'-UTR) of the target mRNA (12). Growing evidence has shown that miRNAs play crucial roles in tumor biological functions, including cell proliferation, differentiation, angiogenesis and invasion (13,14). Previous reports have indicated that miRNAs are dysregulated in several cancer types, including NSCLC (15-18).

miR-103, a member of the miR-103/107 family, is capable of triggering EMT of mammary epithelial cells (19,20). miR-103 functions as an oncogene in several types of cancer, including gastric cancer, hepatocellular carcinoma, colorectal cancer and prostate cancer (21-24). Nevertheless, the role of miR-103 in NSCLC is not fully understood and, to the best of our knowledge, there are no reports on the correlation between miR-103 and EMT in NSCLC. Therefore, the present study focused on investigating the molecular pathways underlying the development and progression of NSCLC, with the aim of identifying potential new targets for diagnosis and treatment.

Materials and methods

Cell culture. Human NSCLC cell lines A549, H1299 and H460, and the human normal lung cell line 16HBE were obtained from the American Type Culture Collection. The cells were cultured in RPMI-1640 medium (Invitrogen;

Thermo Fisher Scientific, Inc.) containing 10% fetal bovine serum (FBS; Gibco; Thermo Fisher Scientific, Inc.) and 1% penicillin/streptomycin with 5% CO_2 at 37˚C.

MTT and colony formation assays. Cell proliferation was assessed using MTT and colony formation assays. For the MTT assay, A549, H1299, H460 and 16HBE cells were seeded at a density of $1x10^4$ cells/well in 96-well plates for 0, 24, 48 and 72 h. MTT (20 μl, 5 mg/ml) was then added to each well at the indicated times and incubated for 4 h at 37˚C. Subsequently, MTT solution was removed and replaced with 150 μl DMSO. The cell viability was measured using a SpectraMax M5 microplate reader (Molecular Devices) at 570 nm. For the colony formation assay, A549, H1299, H460 and 16HBE cells ($1x10^3$ cells/well) were seeded in 6-well plates and cultured for 14 days at 37˚C in a humidified incubator with 5% CO_2. Following two washes with PBS, the cells were fixed with 4% paraformaldehyde at room temperature for 30 min and stained with 0.5% crystal violet for 4 h at room temperature. Cell colonies were counted and photographed using a light microscope (magnification, x40).

5-Ethynyl-2'-deoxyuridine (EdU) assay. A total of $1x10^4$ A549 and H1299 cells/well were plated in a 96-well plate and cultured for 24 h at 37˚C with 5% CO_2. EdU (100 μl; 50 μM) was then added and incubated for a further 2 h, followed by fixing with 4% paraformaldehyde for 20 min. The cells were stained using Cell-Light™ EdU Apollo®488 *In Vitro* Imaging kit (cat. no. C10310-3; Guangzhou RiboBio Co., Ltd.) and DAPI, according to the manufacturer's instructions. EdU-positive cells were detected under a fluorescence microscope (magnification, x400).

Reverse transcription-quantitative PCR (RT-qPCR). Total RNA of cells was extracted using TRIzol reagent (Invitrogen; Thermo Fisher Scientific, Inc.) according to the manufacturer's instructions, and the high-quality RNA was confirmed by ultraviolet analysis and the detection of formaldehyde denaturation electrophoresis. cDNA was synthesized using One Step PrimeScript miRNA cDNA Synthesis kit (Takara Biotechnology Co., Ltd.) at 37˚C for 15 min. qPCR was performed using SYBR Premix Ex Taq (Takara Biotechnology Co., Ltd.) in an ABI 7500 Real-Time PCR system (Applied Biosystems; Thermo Fisher Scientific, Inc.). The qPCR program was as follows: 95˚C for 5 min; followed by 40 cycles of 95˚C for 10 sec, and 60˚C for 30 sec. The gene-specific primer sequences were as follows: miR-103 forward, 5'-AGC AGCATTGTACAGGGCTATCA-3' and reverse, 5'-GCC GTCGGTGATGCTTTTTGG-3'; U6 forward, 5'-GCTTCG GCAGCACATATACTAAAAT-3' and reverse, 5'-CGCTTC ACGAATTTGCGTGTCAT-3'; KLF7 forward, 5'-AGACAT GCCTTGAATTGGAACG-3' and reverse, 5'-GGGGTCTAA GCGACGGAAG-3'; E-cadherin forward, 5'-TACGCCTGG GACTCCACCTA-3' and reverse, 5'-CCAGAAACGGAG GCCTGAT-3'; N-cadherin forward, 5'-CGAGCCGCCTGC GCTGCCAC-3' and reverse, 5'-CGCTGCTCTCCGCTCCC CGC-3'; Vimentin forward, 5'-TACAGGAAGCTGCTGGA AGG-3' and reverse, 5'-ACCAGAGGGAGTGAATCCAG-3'; Snail forward, 5'-TGTTGCAGTGAGGGCAAGAA-3' and reverse, 5'-GACCCTGGTTGCTTCAAGGA-3'; Wnt forward, 5'-ATCCTGCACCTGCGACTACAG-3' and reverse, 5'-GGC

GACTTCTCGAAGTAG-3'; β-catenin forward, 5'-AAGTTC TTGGCTATTACGACA-3' and reverse, 5'-ACAGCACCT TCAGCACTCT-3'; and GAPDH forward, 5'-CAAATTCCA TGGCACCGTCA-3' and reverse, 5'-GGAGTGGGTGTCGCT GTTG-3'. U6 and GAPDH were used as negative controls. The relative expression levels were normalized to GAPDH or U6 using the $2^{-\Delta\Delta Cq}$ method (25).

Western blotting analysis. Total proteins from cells were extracted using radioimmunoprecipitation assay buffer (Thermo Fisher Scientific, Inc.) and the protein concentrations were measured using BCA Protein assay kit. An equal amount of proteins (50 μg) were separated by 10% SDS-PAGE, and then transferred to polyvinylidene difluoride membranes, which were blocked with 5% skim milk in TBS with 1% Tween-20 for 90 min at 25˚C. Subsequently, the membranes were probed with primary antibodies at 4˚C overnight, followed by incubation with secondary antibodies for a further 2 h at room temperature. The following primary antibodies were obtained from Abcam: KLF7 (cat. no. ab80151; 1:1,000), cyclin D1 (cat. no. ab134175; 1:1,000), cyclin-dependent kinase inhibitor 1 p21 (cat. no. ab109520; 1:1,000), p27 (cat. no. ab32034; 1:1,000), Bax (cat. no. ab182733; 1:1,000), Bcl-2 (cat. no. ab32124; 1:1,000), caspase-3 (cat. no. ab13847; 1:500), caspase-9 (cat. no. ab65608; 1:500), cleaved caspased-3 (cat. no. ab49822; 1:1,000), cleaved caspase-9 (cat. no. ab2324; 1:1,000), matrix metallopeptidase (MMP)-2 (cat. no. ab37150; 1:800), MMP-9 (cat. no. ab134455; 1:800), E-cadherin (cat. no. ab40772; 1:1,000), N-cadherin (cat. no. ab202030; 1:1,000), Vimentin (cat. no. ab8978, 1:1,000), Snail (cat. no. ab53519; 1:1,000), Wnt (cat. no. ab219412; 1:1,000), β-catenin (cat. no. ab32572; 1:1,000) and GAPDH (cat. no. ab8245; 1:1,000). Goat anti-mouse/rabbit IgG conjugated to horseradish peroxidase were used as the secondary antibody (cat. no. CW0103 and CW0110S; 1:1,000; CWBio). The immunoreactive bands were visualized using an Enhanced Chemiluminescence Detection system (Thermo Fisher Scientific, Inc.). The blots were analyzed using ImageJ 1.48u software (National Institutes of Health). GAPDH was used as the loading control.

Wound healing assay. A549 and H1299 cells ($1x10^4$/well) were seeded in a 6-well plate and grown to 100% confluence. Scratches were then generated with a 10 μl pipette tip in each well and floating cells were removed by washing with serum-free medium. The wounded monolayers were further cultured in serum-free medium for 24 h. Cell migration was observed and photographed at 0, 24 and 48 h under a light microscope (magnification, x100).

Transwell assay. The migratory and invasive abilities of A549 and H1299 cells were assessed by a Transwell assay. Cells ($5x10^4$) in serum-free medium were added to the upper chamber of Transwell inserts. The bottom chamber was filled with medium with 20% FBS. For invasion analysis, the upper chamber of the inserts was also pre-coated with Matrigel (BD Biosciences) at 37˚C for 4 h. After 24 h, cells that had migrated or invaded to the lower chamber were fixed with 4% paraformaldehyde for 20 min and stained with crystal violet for 4 h at room temperature. Cells were counted and photographed under a light microscope (magnification, x100).
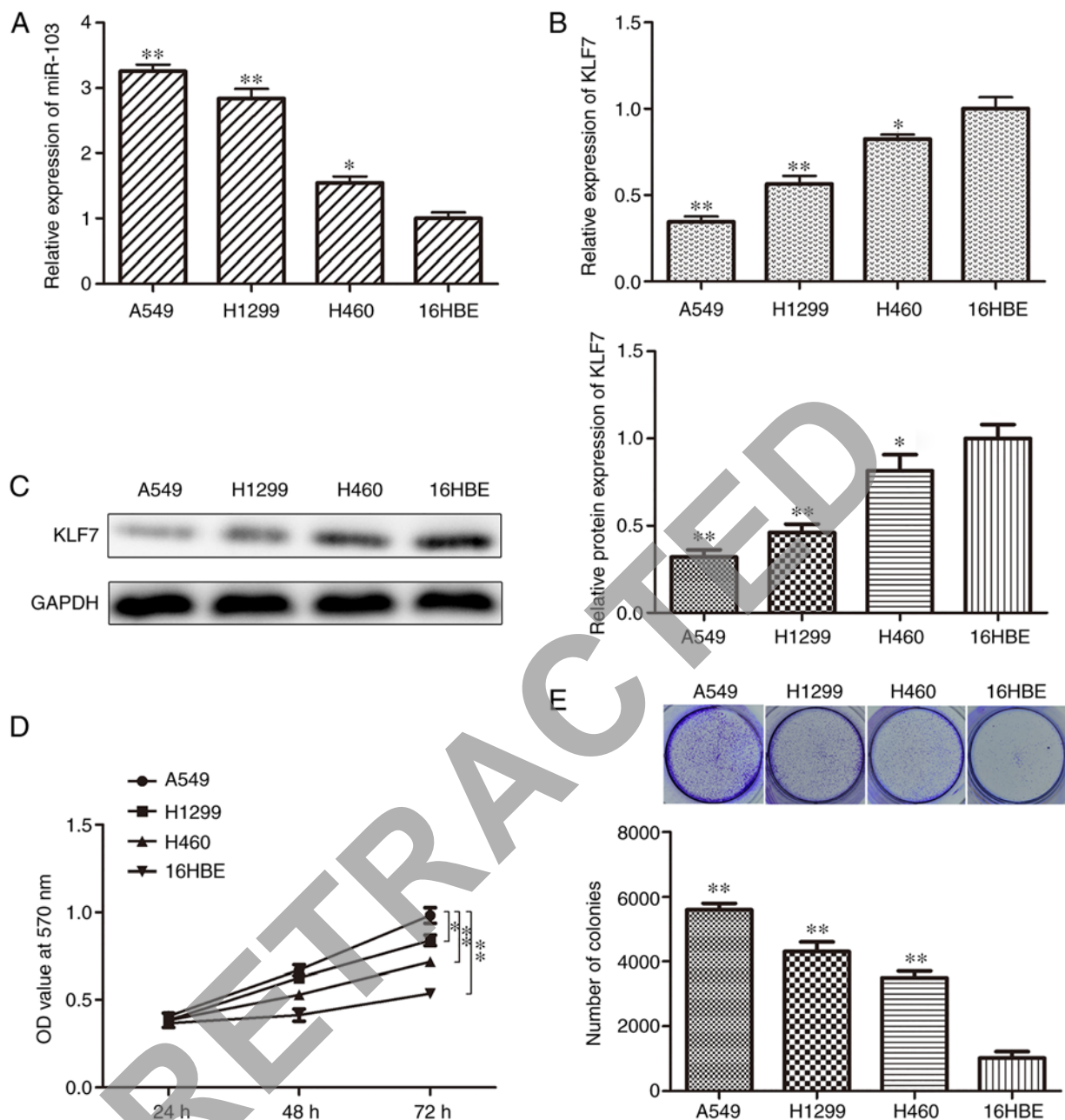
Figure 1. miR-103 is highly expressed in NSCLC cell lines. (A) The expression levels of miR-103 in NSCLC cell lines and the 16HBE cell line were examined by RT-qPCR. *P<0.05, **P<0.01 vs. 16HBE cells. The expression of KLF7 was detected by (B) RT-qPCR and (C) western blot assay in NSCLC cells and 16HBE cells. (D) Proliferation and (E) colony formation ability of cells were determined by MTT and colony formation assays, respectively. Data are presented as the mean ± standard deviation (n=3). *P<0.05, **P<0.01 vs. 16HBE cells. miR-103, microRNA-103; NSCLC, non-small cell lung cancer; RT-qPCR, reverse transcription-quantitative PCR; KLF7, Kruppel-like factor 7; OD, optical density.

Flow cytometric analysis. Flow cytometry was performed to assess the effects of miR-103 on cell cycle progression and apoptosis. For cell cycle analysis, $1x10^6$ A549 and H1299 cells/well were seeded into 6-well plates and incubated overnight. Following transfection for 48 h, cells were collected and washed for three times with FACS buffer (PBS supplemented with 2% FBS). Subsequently, the cells were fixed with 70% cold ethanol overnight at 20˚C, followed by treatment with RNaseA (Sigma-Aldrich; Merck KGaA) for 30 min at 37˚C, and incubation with 20 μg/ml propidium iodide (PI; Sigma-Aldrich; Merck KGaA) for 20 min at room temperature. The cells were then washed with PBS and resuspended in the Cell Cycle Reagent (EMD Millipore). For cell apoptosis analysis, cells

were collected and washed in cold PBS. Subsequently, cells were stained with Annexin V-FITC/PI Apoptosis Detection kit (BD Biosciences) for 15 min at room temperature. All cells were analyzed using a BD FACSCanto II flow cytometer (BD Biosciences) and the results were analyzed using FlowJo 10.0.06 software (FlowJo LLC). The quadrants Q2 and Q3 were used to calculate the apoptosis rate.

Dual-luciferase reporter assay. TargetScan 7.2 (http://www.targetscan.org) and MiRanda 2010 (http://www.microrna.org/microrna/) were used to predict the target of miR-103. It was identified that the 3'-UTR of KLF7 binds to miR-103 with the highest score, suggesting KLF7 may be a target of miR-103.
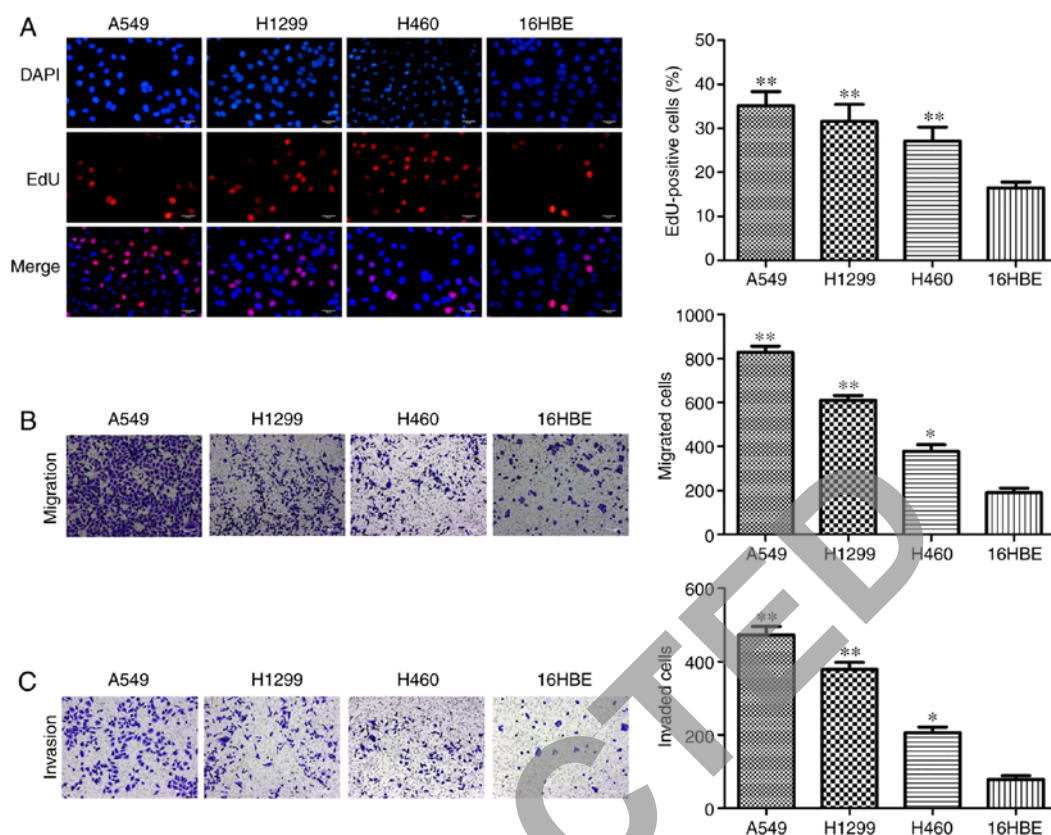
Figure 2. Proliferation, migration and invasion of NSCLC cell lines. (A) Proliferation of cells was determined by EdU assay. Magnification, x400. Scale bar, 50 µm. The (B) migration and (C) invasion of NSCLC cells and 16HBE cells were detected by Transwell assays. Magnification, x100. Scale bar, 100 µm. *P<0.05, **P<0.01 vs. 16HBE cells. NSCLC, non-small cell lung cancer; EdU, 5-ethynyl-2'-deoxyuridine.

For luciferase activity analysis, wild-type or mutant 3'-UTR of KLF7 was cloned into the psicheck-2 vector (Promega Corporation). A549 and H1299 cells were co-transfected with miR-103 mimics, *Renilla* luciferase plasmid and wild-type or mutant 3'-UTR-KLF7 using Lipofectamine 2000 (Promega Corporation). After transfection for 48 h, luciferase activity was measured using dual-luciferase reporter assay system (cat. no. E1910; Promega Corporation), according to the manufacturer's protocol.

Statistical analysis. All results are presented as the mean ± standard deviation, and each experiment was performed with at least three independent replicates. GraphPad Prism 5.0 (GraphPad Software, Inc.) was used to perform the statistical analysis. Statistical differences between means among multiple groups were analyzed by one-way ANOVA followed by Bonferroni's post hoc analysis. P<0.05 was considered to indicate a statistically significant difference.

Results

miR-103 is upregulated in NSCLC cell lines. To improve understanding of whether miR-103 is involved in the progression of human NSCLC, miR-103 expression levels were determined in NSCLC cell lines. RT-qPCR analysis indicated that miR-103 expression was significantly higher in A549, H1299 and H460 cell lines compared with the 16HBE cell line (Fig. 1A). In addition, the expression of KLF7 was also investigated using RT-qPCR and western blotting assays. The data indicated that

KLF7 expression was significantly decreased in the NSCLC cell lines compared with the 16HBE cell line (Fig. 1B and C). MTT, colony formation, EdU and Transwell assays were employed to assess cell proliferation, migration and invasion. The cell proliferation of A549, H1299 and H460 cells was significantly higher compared with 16HBE cells (Fig. 1D). In addition, the colony formation assay indicated that there were indecently more colonies in A549, H1299 and H460 cells compared with 16HBE cells (Fig. 1E). Furthermore, the results of EdU assay demonstrated that A549, H1299 and H460 cells had higher percentages of EdU-positive cells compared with 16HBE cells (Fig. 2A). As presented in Fig. 2B and C, increased migration and invasion rates were observed in A549, H1299 and H460 cells compared with 16HBE cells. These results indicated that miR-103 is significantly increased in NSCLC and NSCLC cells have a higher rate of proliferation, migration and invasion, therefore miR-103 may be associated with the progression of human NSCLC.

miR-103 promotes the viability and proliferation of NSCLC cells. As miR-103 was highly expressed in NSCLC cells, it was hypothesized that miR-103 may be involved in NSCLC. Thus, transfections were performed with miR-103 mimic or miR-103 inhibitor to increase or reduce miR-103 expression in A549 and H1299 cells. RT-qPCR confirmed that miR-103 expression was significantly increased and decreased in A549 and H1299 cells transfected with miR-103 mimic and inhibitor, respectively (Fig. 3A). Furthermore, MTT, colony formation and EdU assays were performed to assess the influence of
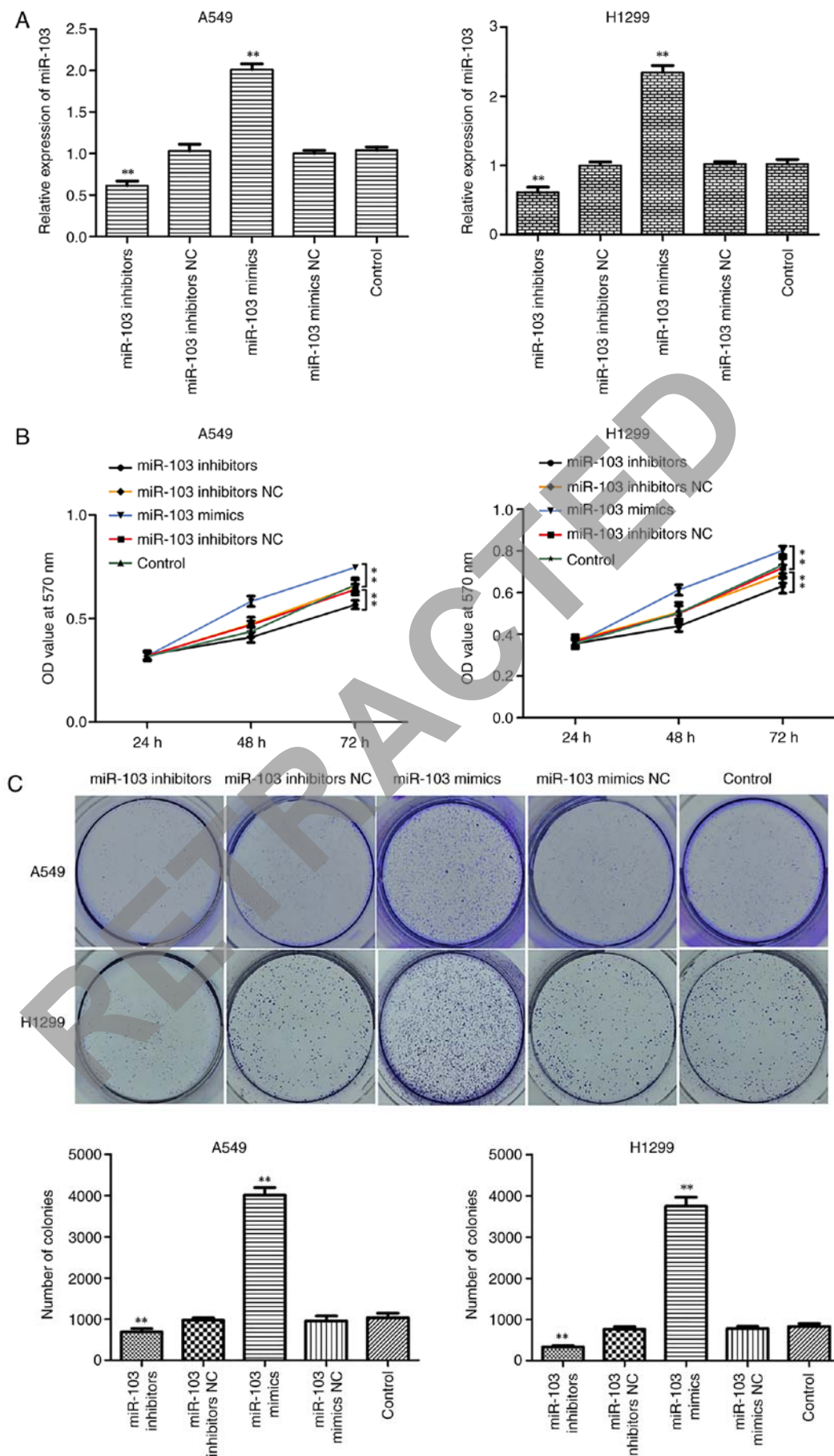
Figure 3. miR-103 promotes cell viability in non-small cell lung cancer. (A) miR-103 expression levels in cell lines transfected with miR-103 mimic and miR-103 inhibitor were measured by reverse transcription-quantitative PCR assay. [**]P<0.01 vs. control. (B) Cell proliferation was assessed by a MTT assay. [**]P<0.01. (C) Colony formation assay was performed with transfected A549 and H1299 cells. Magnification, x400.
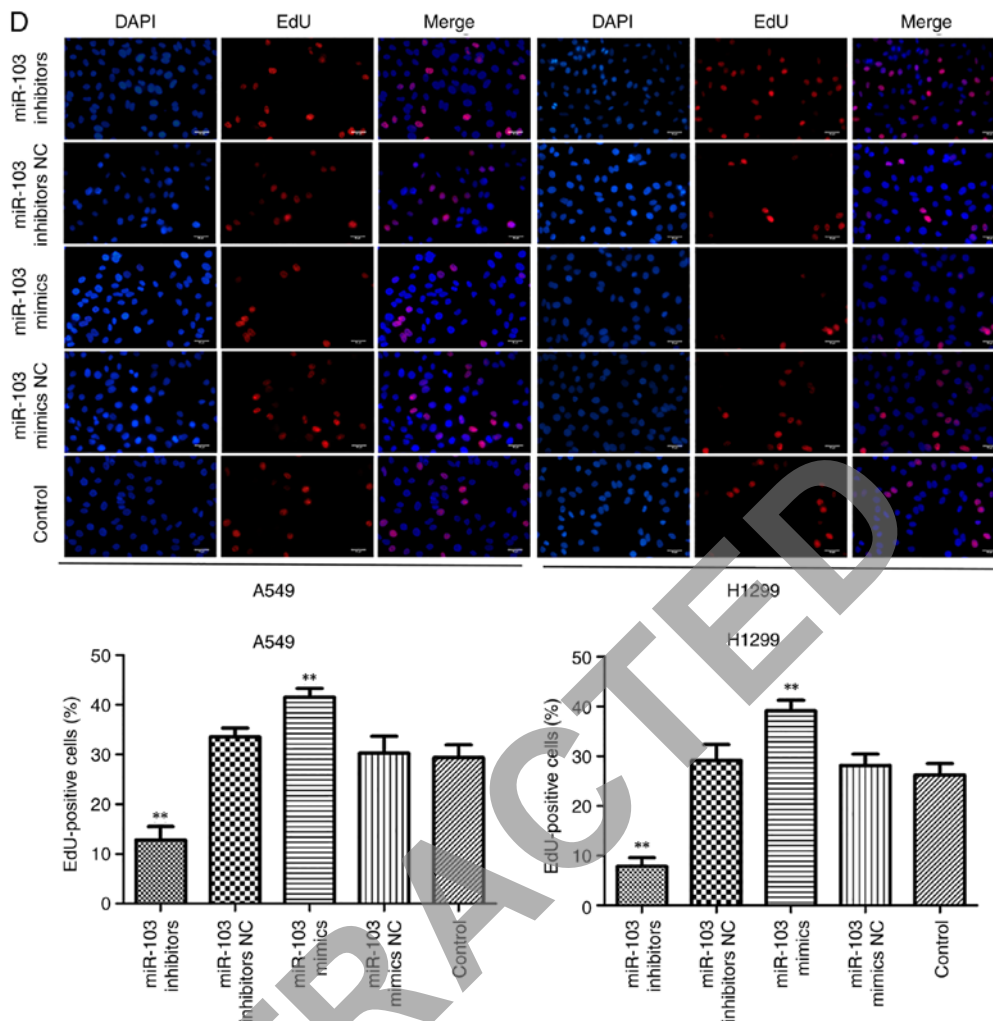
Figure 3. Continued. miR-103 promotes cell viability in non-small cell lung cancer. (D) EdU assay was performed with transfected A549 and H1299 cells. Scale bar, 50 µm. **P<0.01 vs. control. miR-103, microRNA-103; NC, negative control; EdU, 5-ethynyl-2'-deoxyuridine; OD, optical density.

miR-103 on cell viability and proliferation (Fig. 3B-D). As presented in Fig. 3B, miR-103 inhibitor significantly inhibited the growth of A549 and H1299 cells compared with control group, whereas miR-103 mimic significantly promoted cell viability. Colony formation assay revealed that miR-103 mimic significantly increased colony formation, whereas miR-103 inhibitor significantly suppressed colony formation compared with control group (Fig. 3C). Similar results were observed for cell proliferation, as determined by EdU assay (Fig. 3D).

Effects of miR-103 on cell cycle and apoptosis in NSCLC. To investigate the role of miR-103 in NSCLC progression, flow cytometric analysis and western blotting were used to determine the effect of miR-103 on the cell cycle and apoptosis. As presented in Fig. 4A, the cells transfected with miR-103 inhibitor exhibited a significantly increased proportion of cells in the G1 phase. Conversely, upregulation miR-103 resulted in a significant decrease of the cell population in the G1 phase. Furthermore, the cell cycle-related proteins (p21, p27 and cyclin D1) were measured using western blotting (Fig. 4B). Compared with the control cells, the expression level of cyclin D1 was significantly increased, whereas p21 and p27 was significantly decreased in the miR-103 mimic group.

Additionally, cyclin D1 was significantly decreased, and p21 and p27 were significantly increased by miR-103 inhibitor. The results of cell apoptosis analysis demonstrated that over-expression of miR-103 significantly suppressed cell apoptosis, whereas downregulation of miR-103 induced a significant increase in the proportion of apoptotic A549 and H1299 cells when compared with control group (Fig. 5A). Furthermore, the expression levels of apoptosis-related proteins, including Bax, Bcl-2, caspase-3 and caspase-9, were determined in A549 and H1299 cells by western blotting. As presented in Fig. 5B, miR-103 mimic significantly increased the protein expression of Bcl-2 and significantly decreased the protein expression levels of Bax, cleaved caspase-3 and cleaved caspase-9 when compared with the control groups. By contrast, significantly decreased protein expression of Bcl-2 and significantly increased expression of Bax, cleaved caspase-3 and cleaved caspase-9 were observed in cells transfected with miR-103 mimic. These findings indicated that miR-103 accelerated the cell cycle and inhibited cell apoptosis of NSCLC cells.

miR-103 promotes the migration and invasion of NSCLC cells. Wound healing and Transwell assays were performed to elucidate the effects of miR-103 on the migration and invasion
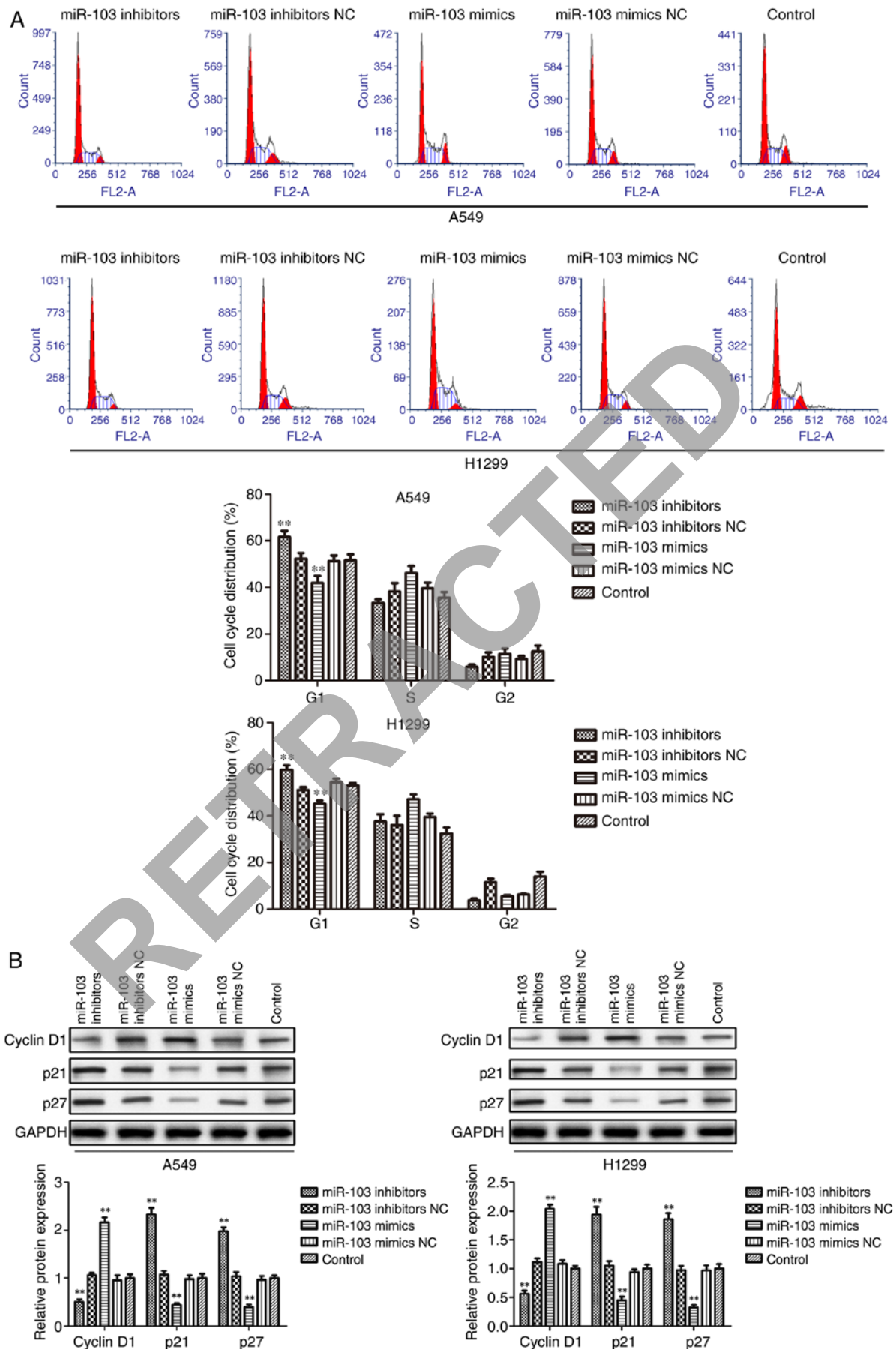
Figure 4. Effect of miR-103 on cell cycle in non-small cell lung cancer. (A) Cell cycle analysis was performed by flow cytometry to determine the impact of miR-103 on cell cycle progression. Overexpression of miR-103 inhibited cell cycle progression, whereas knockdown of miR-103 promoted cell cycle progression. (B) The cell cycle-related proteins p21, p27 and cyclin D1 were measured in A549 and H1299 cells using western blot assays. Data are presented as the mean ± standard deviation (n=3). **P<0.01 vs. control. miR-103, microRNA-103; NC, negative control.
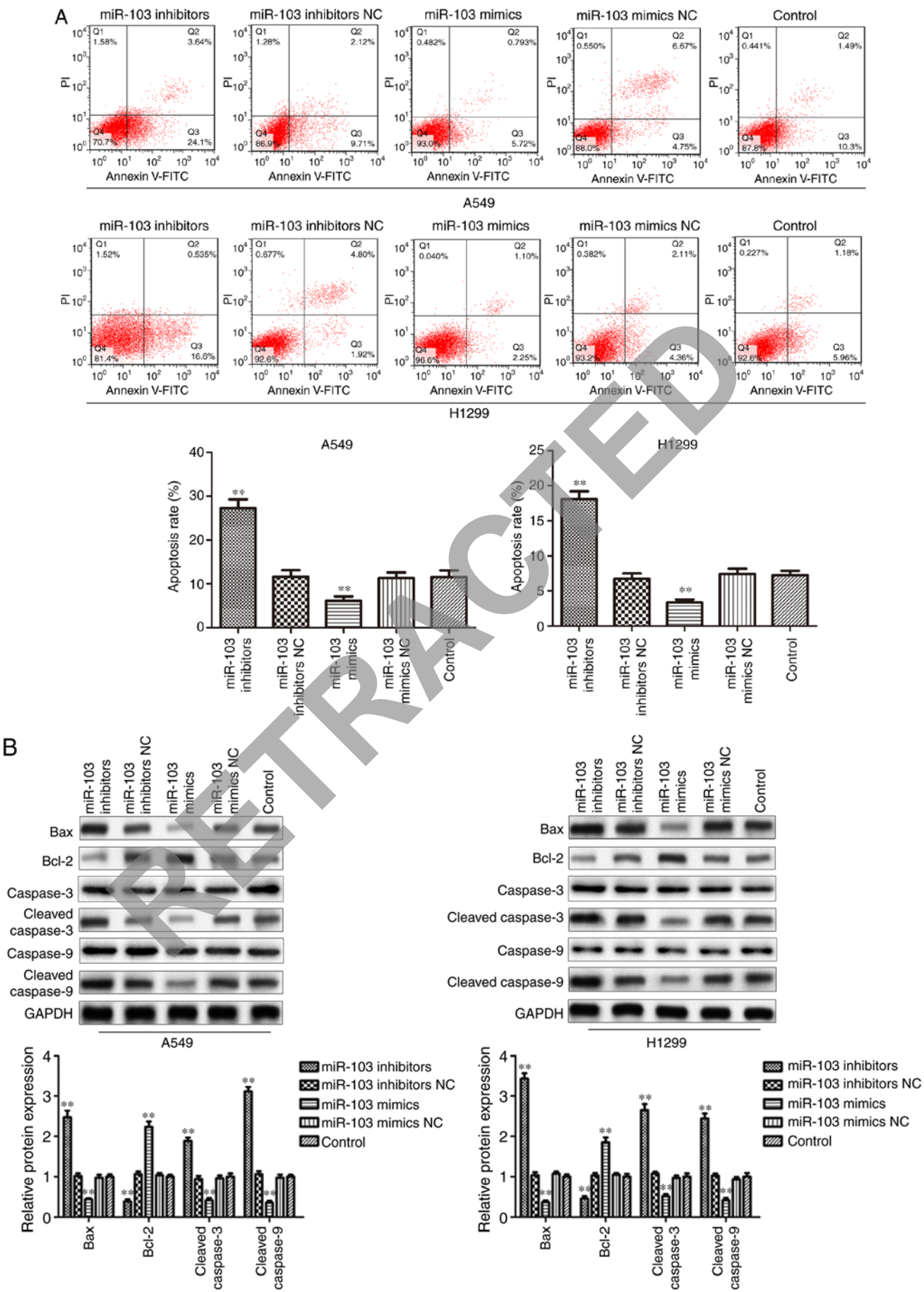
Figure 5. Effect of miR-103 on cell apoptosis in non-small cell lung cancer. (A) Cell apoptosis was analyzed by flow cytometry of A549 and H1299 cells after transfection with miR-103 mimics, miR-103 inhibitors and the NC. (B) Apoptotic proteins were analyzed using western blotting. Data are presented as the mean ± standard deviation (n=3). **P<0.01 vs. control. miR-103, microRNA-103; NC, negative control; PI, propidium iodide.
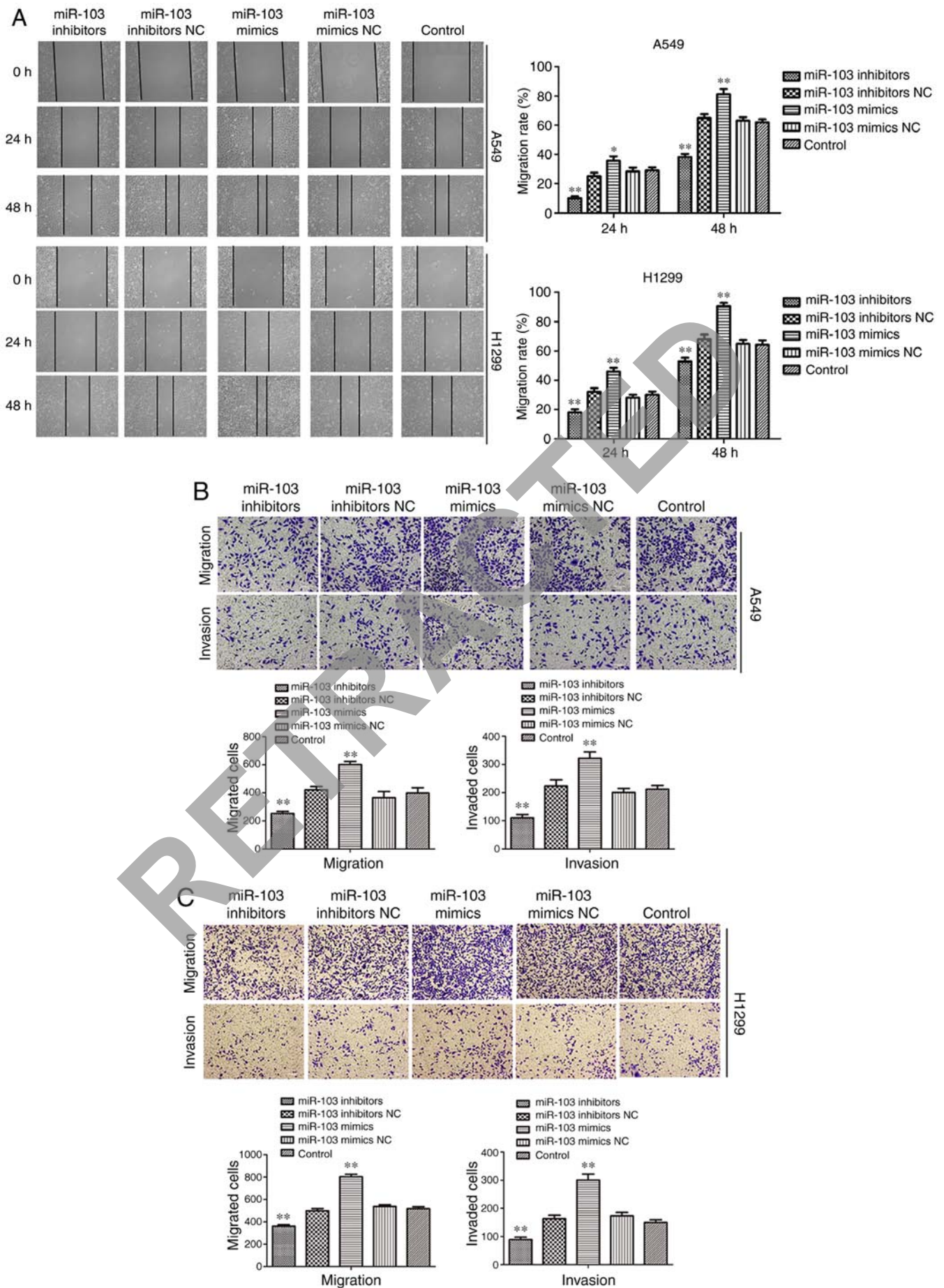
Figure 6. miR-103 promotes cell migration and invasion in NSCLC cells. The migration and invasion of transfected cells were investigated by (A) wound healing and Transwell assays with (B) A549 and (C) H1299 cells. Magnification x100.
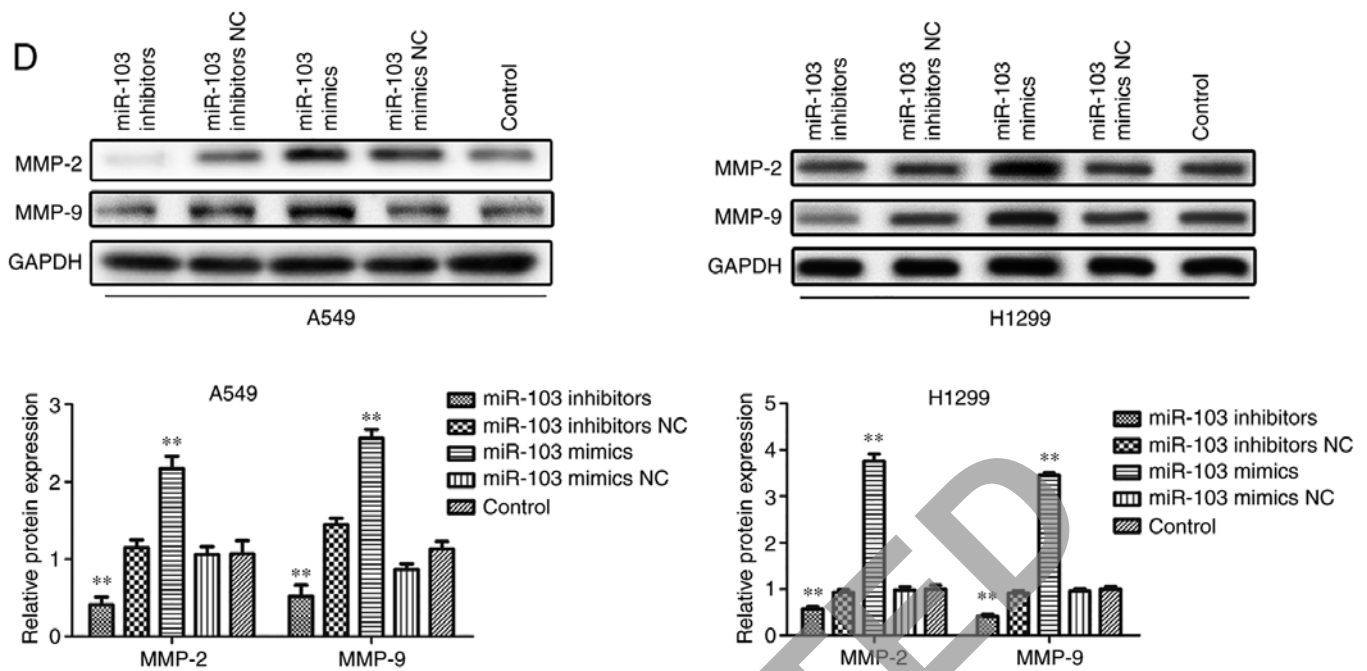
Figure 6. Continued. miR-103 promotes cell migration and invasion in NSCLC cells. (D) The protein expression levels of MMP-2 and MMP-9 in A549 and H1299 cells were measured by western blotting. *P<0.05 and **P<0.01 vs. control. miR-103, microRNA-103; NC, negative control; MMP, matrix metallopeptidase.

of A549 and H1299 cells. As presented in Fig. 6A, cells transfected with miR-103 mimic exhibited a significantly increased migratory rate compared with the control cells, while miR-103 inhibitor decreased the migratory rate. Transwell migration and invasion assays revealed a significant positive effect of miR-103 on the migratory and invasive abilities of A549 and H1299 cells. The results demonstrated that compared with the control cells, the migration and invasion were significantly increased by miR-103 mimic, and miR-103 inhibitor induced the opposite effects (Fig. 6B and C). MMPs participate in cancer cell invasion by degrading the extracellular matrix (26). Therefore, MMP-2 and MMP-9 expression levels were used to elucidate the effect of miR-103 on cell migration and invasion. The data revealed that the expression levels of MMP-2 and MMP-9 were significantly inhibited in cells transfected with miR-103 inhibitors compared with the control group (Fig. 6D). Additionally, miR-103 mimic significantly increased MMP-2 and MMP-9 levels compared with the control group (Fig. 6D).

miR-103 promotes the EMT of NSCLC cells. Furthermore, it was investigated whether miR-103 modulates the EMT of NSCLC cells. As presented in Fig. 7, RT-qPCR and western blot analysis revealed that inhibition of miR-103 significantly promoted the expression of E-cadherin and significantly decreased the expression of N-cadherin, Vimentin and Snail compared with the control group in A549 and H1299 cells. By contrast, the expression of E-cadherin was significantly decreased and the expression levels of N-cadherin, Vimentin and Snail were significantly increased in cells transfected with miR-103 mimic compared with the control group. These data indicated that miR-103 promoted the EMT of NSCLC.

miR-103 suppresses the expression of KLF7 in NSCLC cells by binding to the 3'-UTR of the KLF7 gene. To improve

understanding of the underlying mechanisms of miR-103, bioinformatics tools TargetScan and MiRanda were used to predict the putative target genes of miR-103, and it was identified that KLF-7 may be a target for miR-103. As presented in Fig. 8A, the programs predicted that the sequence of the 3'-UTR of KLF7 had binding sites for miR-103. To confirm whether miR-103 directly binds to the 3'-UTR of KLF7, luciferase reporter vectors containing the wild-type KLF7 3'-UTR and mutated KLF7 3'-UTR sequences were constructed, followed by co-transfection into A549 and H1299 cells together with miR-103 mimic and the negative control (Fig. 8B). The results demonstrated that co-transfection of miR-103 mimic and KLF7 wild-type resulted in significantly decreased luciferase activity, whereas KLF7 mutant did not result in an obvious reduction in luciferase activity, which indicates that miR-103 directly binds to the 3'-UTR of KLF7 (Fig. 8B). As demonstrated by RT-qPCR, western blot and immunofluorescence assays, KLF7 expression was significantly increased in the cell lines transfected with miR-103 inhibitor, and overexpression of miR-103 in A549 and H1299 cells significantly reduced KLF7 mRNA and protein expressions compared with control cells (Fig. 8C-E). Collectively, these data suggested that KLF7 is a direct target of miR-103 in NSCLC.

miR-103 activates the Wnt/β-catenin signaling pathway in NSCLC. To further clarify the underlying molecular mechanisms of miR-103 in NSCLC cells, the expression levels of Wnt and β-catenin were examined using RT-qPCR and western blotting following transfection of A549 and H1299 cells. As presented in Fig. 9, miR-103 inhibitor significantly inhibited the mRNA and protein expression levels of Wnt and β-catenin compared with the control group. In comparison, miR-103 mimic significantly enhanced the expression levels of Wnt and β-catenin in A549 and H1299 cells. These observations suggested that miR-103
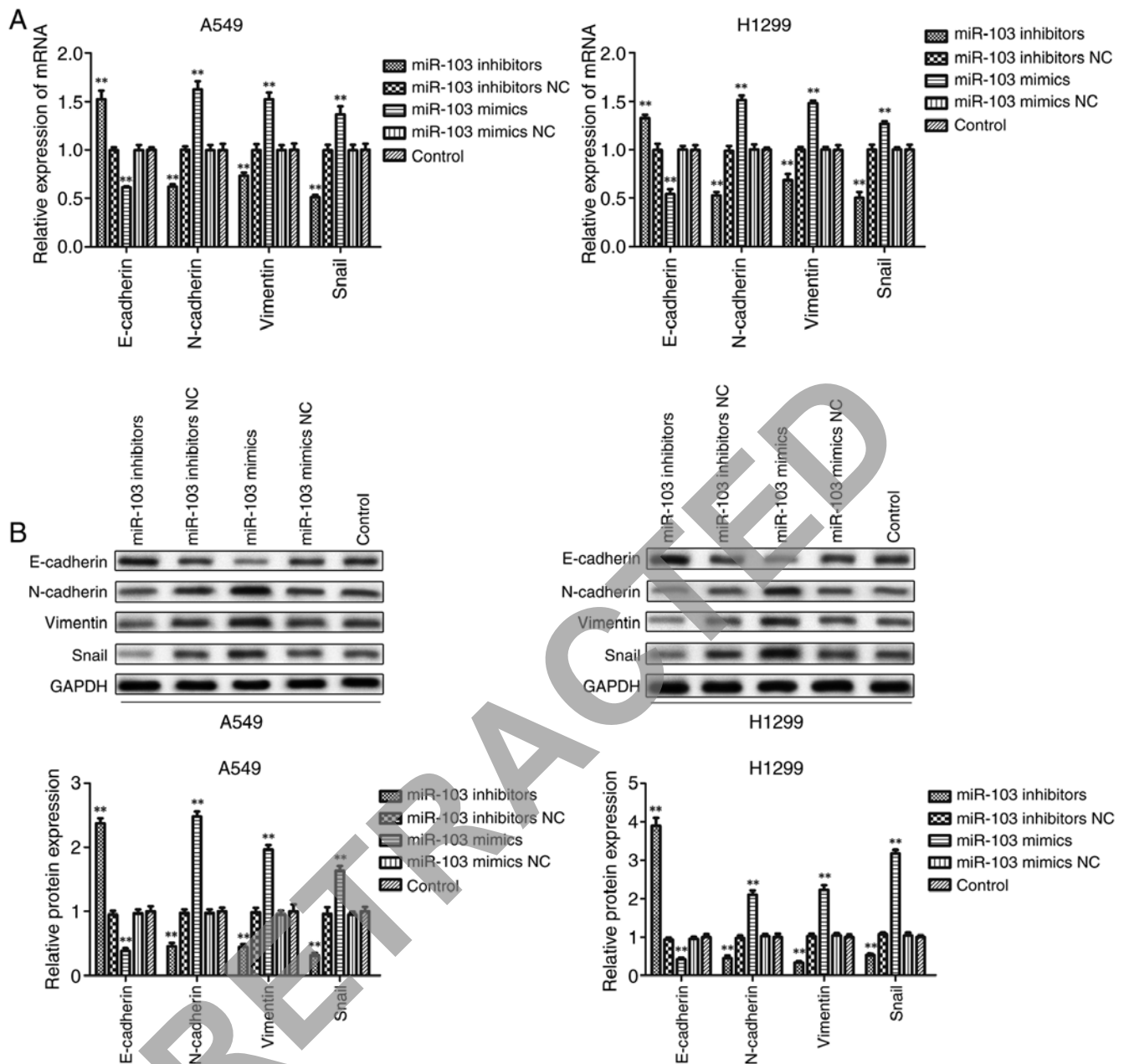
Figure 7. miR-103 promotes the epithelial-mesenchymal transition of non-small cell lung cancer cells. The expression levels of E-cadherin, N-cadherin, Vimentin and Snail in A549 and H1299 cells were measured by (A) reverse transcription-quantitative PCR and (B) western blot analysis. GAPDH served as a loading control. **P<0.01 vs. control. miR-103, microRNA-103; NC, negative control.

may be involved in the regulation of cell biological function, partly via the Wnt/β-catenin signaling pathway in NSCLC.

Discussion

Lung cancer is the most frequent malignancy and is the leading cause of cancer-associated mortality worldwide (27). The identification of miRNAs and their targets in NSCLC progression may provide promising therapeutic opportunities. Increasing evidence has demonstrated that miRNAs exhibit important functions in human malignant tumor development and metastasis by targeting downstream genes, including in NSCLC (28-35). Aberrant expression of miR-103 has been confirmed in colorectal cancer, esophageal cancer, pancreatic

cancer and breast cancer (36-40). However, the biological role of miR-103 in NSCLC requires further investigation.

Although the roles of numerous miRNAs in malignant tumors have been reported, little research has revealed the function of miR-103 on tumor progression (41). miR-103 has been reported to have a tumor suppressor effect on NSCLC (42), however, to the best of our knowledge, a comprehensive assessment of the effects of miR-103 on all processes in NSCLC cells has not been performed. Previous studies have focused on the role of miR-103 in the process of apoptosis (43,44), however they did not elaborate on other processes. Therefore, the present study investigated other functions of miR-103 in the tumorigenic processes of NSCLC. In addition, the current study demonstrated that the novel target KLF7 mediates the
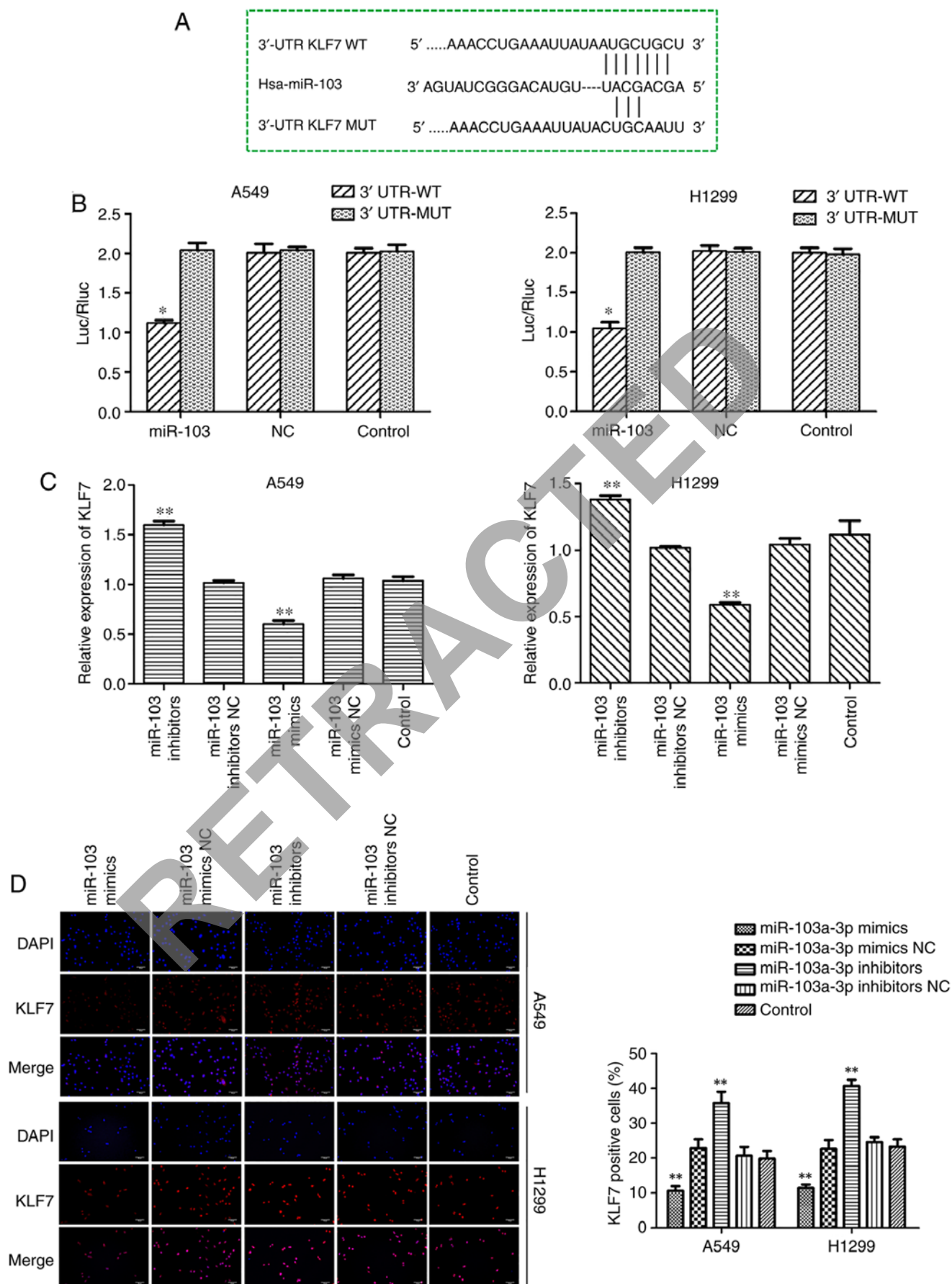
Figure 8. miR-103 suppresses the expression of KLF7 in NSCLC cells by binding to the 3'-UTR of the KLF7 gene. (A) miR-103 and its putative binding sequence in the 3'-UTR of KLF7. (B) A dual-luciferase reporter assay was performed to further confirm whether miR-103 can directly target the 3'-UTR region of KLF7 in NSCLC cells. *P<0.05 vs. 3'-UTR-MUT. The expression levels of KLF7 in A549 and H1299 cells transfected with miR-103 mimic or inhibitor were measured by (C) reverse transcription-quantitative PCR and (D) western blot analysis. **P<0.01 vs. control.
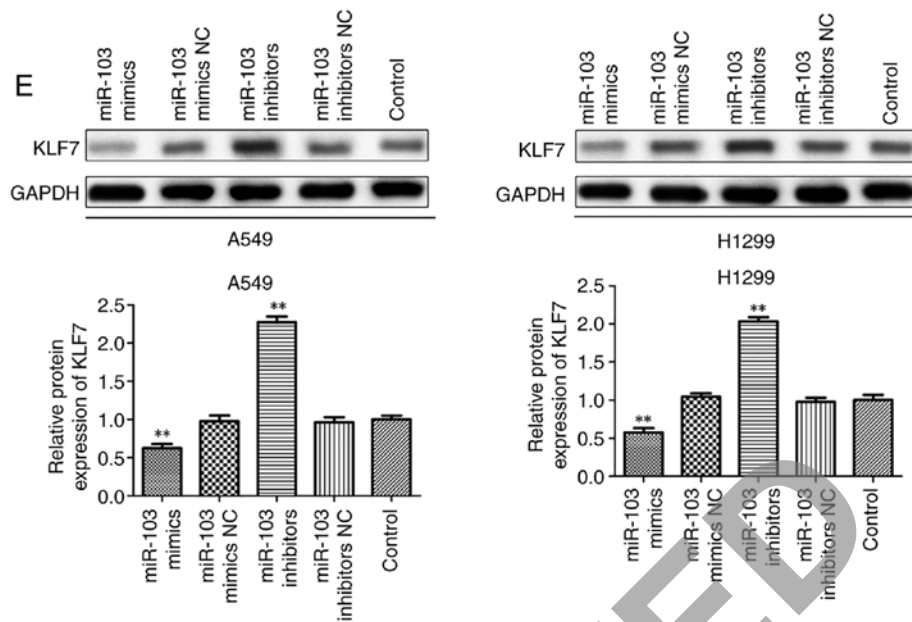
Figure 8. Continued. miR-103 suppresses the expression of KLF7 in NSCLC cells by binding to the 3'-UTR of the KLF7 gene. (E) The expression of KLF7 regulated by miR-103 in A549 and H1299 cells was assessed by immunofluorescence analysis. Magnification, x200. Scale bar, 50 μm. **P<0.01 vs. control. miR-103, microRNA-103; NC, negative control; KLF7, Kruppel-like factor 7; 3'-UTR, 3'-untranslated region; NSCLC, non-small cell lung cancer; Luc, luciferase; Rluc, *Renilla* luciferase; WT, wild-type; MUT, mutant.
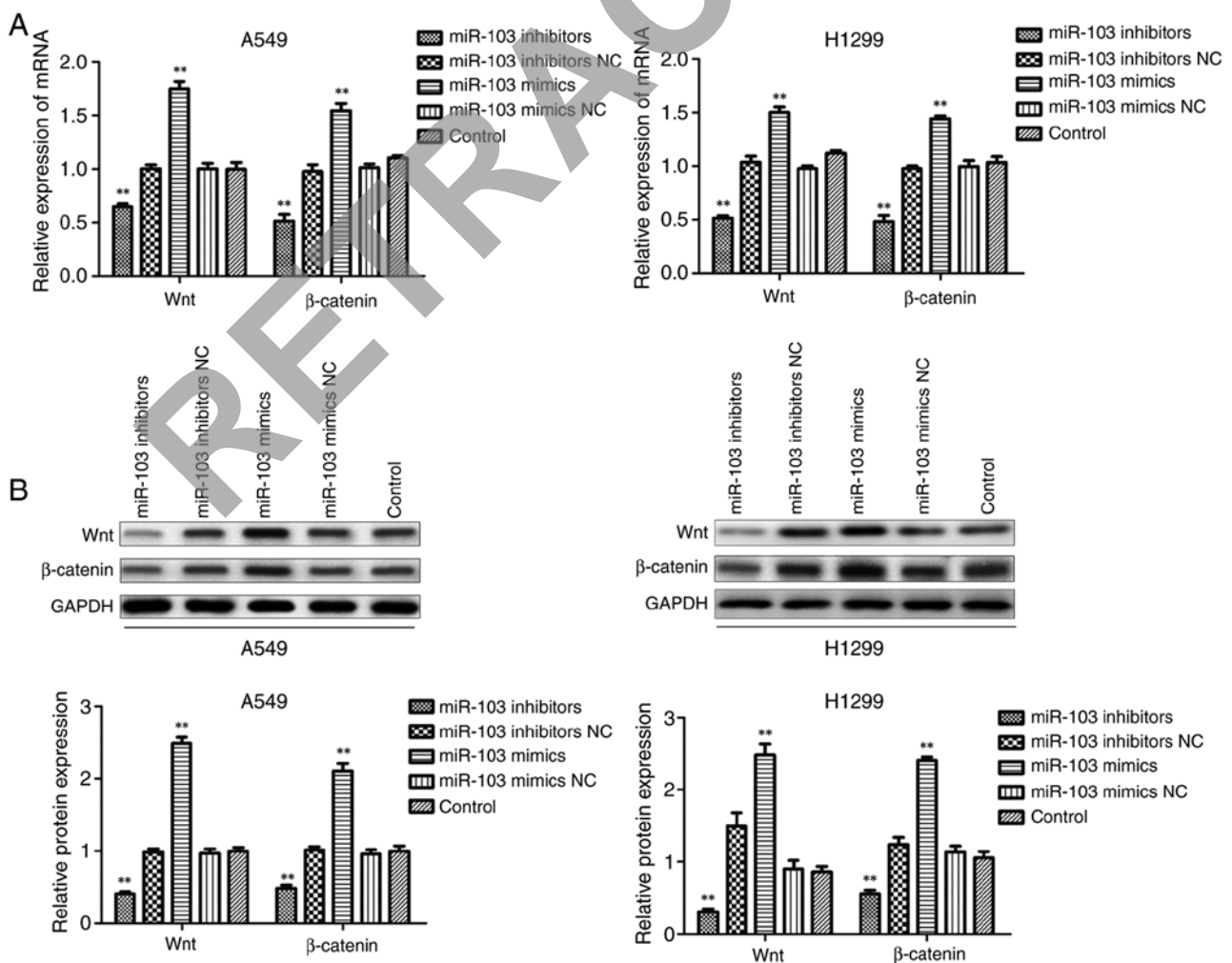

Figure 9. miR-103 activates the Wnt/β-catenin signaling pathway in non-small cell lung cancer cells. The (A) mRNA and (B) protein expression levels of Wnt and β-catenin were determined in transfected A549 and H1299 cells. Data are presented as the mean ± standard deviation. **P<0.01 vs. control. miR-103, microRNA-103; NC, negative control.

role of miR-103. The function of KLF7 in the regulatory effects of miR-103 in NSCLC is clearly greater than that reported for PDCD10 (45,46). RT-qPCR and western blot analysis showed the expression of KLF4 protein was increased in the cell lines transfected with miR-103 inhibitor. As previously reported, *KLF4* is a proliferation-and metastasis-associated gene in cancer (47). Therefore, the target KLF7 is an effective factor in inhibiting NSCLC (48,49). A comprehensive systematic evaluation of miR-103 to determine its functions and the most direct effector molecules is beneficial for the identification of targeted therapies and drug development.

The present study demonstrated that miR-103 was significantly overexpressed in NSCLC cells. Therefore, it was hypothesized that miR-103 may serve a key role in the development of NSCLC, and subsequent functional assays were performed. The results suggested that increased expression of miR-103 significantly promoted cell viability, proliferation, migration and invasion, and inhibited the apoptosis of A549 and H1299 cells. Furthermore, downregulation of miR-103 attenuated the growth, migration and invasion of NSCLC cells, and increased the apoptosis. These findings indicated that miR-103 may act as a tumor oncogene and downregulation of its expression may inhibit the progression of NSCLC.

EMT is a pathological process implicated in tumor progression (50). Cells switch from a polarized, immobile epithelial phenotype to a highly mobile fibroblastic or mesenchymal phenotype in EMT, which involves the loss of epithelial cell markers and the expression of mesenchymal cell markers (51-53). In the present study, downregulation of miR-103 could increase the expression level of E-cadherin and decrease the expression levels of N-cadherin, Vimentin and Snail compared with control A549 and H1299 cells. These data indicated that miR-103 promotes EMT of NSCLC cells.

miRNAs, a class of endogenous RNA, can regulate protein expression by inhibiting or inducing the degradation of mRNAs through specifically binding to the 3'-UTRs (54,55). One miRNA may act on a variety of target genes or proteins, and its target genes and biological roles may vary in different tissues or cells (56). Based on computer information programs or predictive software, bioinformatics in combination with genome sequencing work and clinical-related information can be adapted for different research purposes and/or analytical methods of researchers (57,58). In the current study, KLF7 was predicted as one of direct targets of miR-103. KLF7 is a member of the KLF family, which are transcription factors that belong to the zinc-finger family (59). KLFs regulate diverse cellular processes, including cell proliferation, differentiation, adipogenesis and metabolism (60-62). The present study used a dual-luciferase reporter assay, western blotting, RT-qPCR and immunofluorescence to identify that KLF7 is a direct target of miR-103 in NSCLC. Furthermore, numerous studies have shown that abnormal activation of the Wnt/β-catenin signaling pathway is associated with cancer tumorigenesis and metastasis (63-67). The present data demonstrated that inhibition of miR-103 expression significantly increased the expression levels of Wnt and β-catenin, which are markers of the Wnt signaling pathway (68). Therefore, the current study provides a basis for future investigations of the functions of miR-103 as a critical regulator of the Wnt/β-catenin signaling pathway in NSCLC.

Limitations of the present study included: i) Lack of methods to determine the safety and feasibility of transfecting miR-103 inhibitors and mimics into control cells; and ii) A lack of knockdown experiments to evaluate the association between the Wnt/β-catenin pathway and miR-103. These issues will be addressed in future studies. Taken together, the current study demonstrated that miR-103 is upregulated in NSCLC. Functional assays identified that miR-103 overexpression could promote cell growth, migration and invasion, and inhibit apoptosis in NSCLC. Furthermore, it was demonstrated that KLF7 is a functional target of miR-103. In addition, it was revealed that miR-103 promotes EMT via regulation of the Wnt/β-catenin signaling pathway in NSCLC. In summary, the present study demonstrated that miR-103 functions as a tumor oncogene in NSCLC by targeting KLF7 expression perhaps via the Wnt/β-catenin signaling pathway in NSCLC.

Acknowledgements

Availability of data and materials

The datasets used and/or analyzed during the current study are available from the corresponding author on reasonable request.

Authors' contributions

CY designed the experiments. KL and CY performed the experiments. KL drafted the manuscript. All authors read and approved the final manuscript.

Ethics approval and consent to participate

Not applicable.

Patient consent for publication

Not applicable.

Competing interests

The authors declare that they have no competing interests.

References

1. Bray F, Ferlay J, Soerjomataram I, Siegel RL, Torre LA and Jemal A: Global cancer statistics 2018: GLOBOCAN estimates of incidence and mortality worldwide for 36 cancers in 185 countries. CA Cancer J Clin 68: 394-424. 2018.
2. Duma NR, Santana-Davila R and Molina JR: Non-small cell lung cancer: Epidemiology, screening, diagnosis, and treatment. Mayo Clin Proc 94: 1623-1640, 2019.
3. Ettinger DS, Wood DE, Akerley W, Bazhenova LA, Borghaei H, Camidge DR, Cheney RT, Chirieac LR, D'Amico TA, Demmy TL, *et al*: Non-small cell lung cancer, version 1.2015. J Natl Compr Canc Netw 12: 1738-1761, 2014.

4. Gompelmann D, Eberhardt R and Herth FJ: Advanced malignant lung disease: What the specialist can offer. Respiration 82: 111-123, 2011.

5. Goldstraw P, Chansky K, Crowley J, Porta RR, Asamura H, Eberhardt WE, Nicholson AG, Groome P, Mitchell A, Bolejack V, et al: The IASLC lung cancer staging project: Proposals for revision of the tnm stage groupings in the forthcoming (Eighth) edition of the TNM classification for lung cancer. J Thorac Oncol 11: 39-51, 2016.

6. Choi WI, Lee DY, Choi HG and Lee CW: Lung cancer development and mortality in interstitial lung disease with and without connective tissue diseases: A five-year nationwide population-based study. Respir Res 20: 117, 2019.

7. Sève P, Reiman T and Dumontet C: The role of betaIII tubulin in predicting chemoresistance in non-small cell lung cancer. Lung Cancer 67: 136-143, 2010.

8. Wei S, Zheng Y, Jiang Y, Li X, Geng J, Shen Y, Li Q, Wang X, Zhao C, Chen Y, et al: The circRNA circPTPRA suppresses epithelial-mesenchymal transitioning and metastasis of NSCLC cells by sponging miR-96-5p. EBioMedicine 44: 182-193, 2019.

9. Raoof S, Mulford IJ, Cabanos HF, Nangia V, Timonina D, Labrot E, Hafeez N, Bilton SJ, Drier Y, Ji D, et al: Targeting FGFR overcomes EMT-mediated resistance in EGFR mutant non-small cell lung cancer. Oncogene 38: 6399-6413, 2019.

10. Yang F, Yan Y, Yang Y, Hong X, Wang M, Yang Z, Liu B and Ye L: MiR-210 in exosomes derived from CAFs promotes non-small cell lung cancer migration and invasion through PTEN/PI3K/AKT pathway. Cell Signal 73: 109675, Sep 2020 (Epub ahead of print).

11. Del Vescovo V, Grasso M, Barbareschi M and Denti MA: MicroRNAs as lung cancer biomarkers. World J Clin Oncol 5: 604-620, 2014.

12. Deng S, Calin GA, Croce CM, Coukos G and Zhang L: Mechanisms of microRNA deregulation in human cancer. Cell Cycle 7: 2643-2646, 2008.

13. Tüfekci KU, Meuwissen RL and Genç S: The role of microRNAs in biological processes. Methods Mol Biol 1107: 15-31, 2014.

14. Qian B, Nag SA, Su Y, Voruganti S, Qin JJ, Zhang R and Cho WC: miRNAs in cancer prevention and treatment and as molecular targets for natural product anticancer agents. Curr Cancer Drug Targets 13: 519-541, 2013.

15. Fang C, Chen YX, Wu NY, Yin JY, Li XP, Huang HS, Zhang W, Zhou HH and Liu ZQ: MiR-488 inhibits proliferation and cisplatin sensibility in non-small-cell lung cancer (NSCLC) cells by activating the eIF3a-mediated NER signaling pathway. Sci Rep 7: 40384, 2017.

16. Li T, Ding ZL, Zheng YL and Wang W: MiR-484 promotes non-small-cell lung cancer (NSCLC) progression through inhibiting Apaf-1 associated with the suppression of apoptosis. Biomed Pharmacother 96: 153-164, 2017.

17. Fortunato O, Borzi C, Milione M, Centonze G, Conte D, Boeri M, Verri C, Moro M, Facchinetti F, Andriani F, et al: Circulating mir-320a promotes immunosuppressive macrophages M2 phenotype associated with lung cancer risk. Int J Cancer 144: 2746-2761, 2019.

18. Ni K, Wang D, Xu H, Mei F, Wu C, Liu Z and Zhou B: miR-21 promotes non-small cell lung cancer cells growth by regulating fatty acid metabolism. Cancer Cell Int 19: 219, 2019.

19. Martello G, Rosato A, Ferrari F, Manfrin A, Cordenonsi M, Dupont S, Enzo E, Guzzardo V, Rondina M, Spruce T, et al: A MicroRNA targeting dicer for metastasis control. Cell 141: 1195-1207, 2010.

20. Cai X, Liu Q, Zhang X, Ren Y, Lei X, Li S, Chen Q, Deng K, Wang P, Zhang H and Shi D: Identification and analysis of the expression of microRNA from lactating and nonlactating mammary glands of the Chinese swamp buffalo. J Dairy Sci 100: 1971-1986, 2017.

21. Zheng J, Liu Y, Qiao Y, Zhang L and Lu S: miR-103 promotes proliferation and metastasis by targeting KLF4 in gastric cancer. Int J Mol Sci 18: 910, 2017.

22. Chen HY, Lin YM, Chung HC, Lang YD, Lin CJ, Huang J, Wang WC, Lin FM, Chen Z, Huang HD, et al: miR-103/107 promote metastasis of colorectal cancer by targeting the metastasis suppressors DAPK and KLF4. Cancer Res 72: 3631-3641, 2012.

23. Xue D, Zhou C, Lu H, Xu R, Xu X and He X: LncRNA GAS5 inhibits proliferation and progression of prostate cancer by targeting miR-103 through AKT/mTOR signaling pathway. Tumour Biol 14: 1007, 2016.

24. Xia W, Ni J, Zhuang J, Qian L, Wang P and Wang J: MiR-103 regulates hepatocellular carcinoma growth by targeting AKAP12. Int J Biochem Cell Biol 71: 1-11, 2016.

25. Livak KJ and Schmittgen TD: Analysis of relative gene expression data using real-time quantitative PCR and the 2(-Delta Delta C(T)) method. Methods 25: 402-408, 2001.

26. Poincloux R, Lizárraga F and Chavrier P: Matrix invasion by tumour cells: A focus on MT1-MMP trafficking to invadopodia. J Cell Sci 122: 3015-3024, 2009.

27. Yin Q, Fischer L, Noethling C and Schaefer WR: In vitro-assessment of putative antiprogestin activities of phytochemicals and synthetic UV absorbers in human endometrial ishikawa cells. Gynecol Endocrinol 31: 578-581, 2015.

28. Chen W, Zheng R, Zeng H, Zhang S and He J: Annual report on status of cancer in China, 2011. Chin J Cancer Res 27: 2-12, 2015.

29. Cortinovis D, Monica V, Pietrantonio F, Ceresoli GL, Spina CM and Wannesson L: MicroRNAs in non-small cell lung cancer: Current status and future therapeutic promises. Curr Pharm Des 20: 3982-3990, 2014.

30. Boeri M, Pastorino V and Sozzi G: Role of microRNAs in lung cancer: Microrna signatures in cancer prognosis. Cancer J 18: 268-274, 2012.

31. Vannini I, Fanini V and Fabbri M: MicroRNAs as lung cancer biomarkers and key players in lung carcinogenesis. Clin Biochem 46: 918-925, 2013.

32. Tsang FH, Au SL, Wei L, Fan DN, Lee JM, Wong CC, Ng IO and Wong CM: MicroRNA-142-3p and microRNA-142-5p are down-regulated in hepatocellular carcinoma and exhibit synergistic effects on cell motility. Front Med 9: 331-343, 2015.

33. Chang F, Lee JT, Navolanic PM, Steelman LS, Shelton JG, Blalock WL, Franklin RA and McCubrey JA: Involvement of PI3K/Akt pathway in cell cycle progression, apoptosis, and neoplastic transformation: A target for cancer chemotherapy. Leukemia 17: 590-603, 2003.

34. Osaki M, Oshimura M and Ito H: PI3K-Akt pathway: Its functions and alterations in human cancer. Apoptosis 9: 667-676, 2004.

35. Nicholson KM and Anderson NG: The protein kinase B/Akt signalling pathway in human malignancy. Cell Signal 14: 381-395, 2002.

36. Bader AG, Kang S, Zhao L and Vogt PK: Oncogenic PI3K deregulates transcription and translation. Nat Rev Cancer 5: 921-929, 2005.

37. Yu QF, Liu P, Li ZY, Zhang CF, Chen SQ, Li ZH, Zhang GY and Li JC: MiR-103/107 induces tumorigenicity in bladder cancer cell by suppressing PTEN. Eur Rev Med Pharmacol Sci 22: 8616-8623, 2018.

38. Zheng YB, Xiao K, Xiao GC, Tong SL, Ding Y, Wang QS, Li SB and Hao ZN: MicroRNA-103 promotes tumor growth and metastasis in colorectal cancer by directly targeting LATS2. Oncol Lett 12: 2194-2200, 2016.

39. Zhao BS, Liu G, Wang TY, Ji YH, Qi B, Tao P, Li HC and Wu XN: Screening of microRNA in patients with esophageal cancer at same tumor node metastasis stage with different prognoses. Asian Pac J Cancer Prev 14: 139-143, 2013.

40. Tian Y, Xue Y, Ruan G, Cheng K, Tian J, Qiu Q, Xiao M, Li H, Yang H and Wang L: Interaction of serum microRNAs and serum folate with the susceptibility to pancreatic cancer. Pancreas 44: 23-30, 2015.

41. Zhuan B, Lu Y, Chen Q, Zhao X, Li P, Yuan Q and Yang Z: Overexpression of the long noncoding RNA TRHDE-AS1 inhibits the progression of lung cancer via the miRNA-103/KLF4 axis. J Cell Biochem 120: 17616-17624, 2019.

42. Yang D, Wang JJ, Li JS and Xu QY: miR-103 functions as a tumor suppressor by directly targeting programmed cell death 10 in NSCLC. Oncol Res 26: 519-528, 2018.

43. Zhang Z, Wu S, Muhammad S, Ren Q and Sun C: miR-103/107 promote ER stress-mediated apoptosis via targeting the Wnt3a/β-catenin/ATF6 pathway in preadipocytes. J Lipid Res 59: 843-853, 2018.

44. Wang X, Lin Y, Peng L, Sun R, Gong X, Du J and Zhang X: MicroRNA-103 promotes proliferation and inhibits apoptosis in spinal osteosarcoma cells by targeting p57. Oncol Res 26: 933-940, 2018.

45. Fu X, Zhang W, MSu Y, Lu L, Wang D and Wang H: MicroRNA-103 suppresses tumor cell proliferation by targeting PDCD10 in prostate cancer. Prostate 76: 543-551, 2016.

46. Niu R, Tang Y, Xi Y and Jiang D: High expression of Krüppel-like factor 7 indicates unfavorable clinical outcomes in patients with lung adenocarcinoma. J Surg Res 250: 216-223, 2020.

47. Ma Y, Wu L, Liu X, Xu Y, Shi W, Liang Y, Yao L, Zheng J and Zhang J: KLF4 inhibits colorectal cancer cell proliferation dependent on NDRG2 signaling. Oncol Rep 38: 975-984, 2017.
48. Zhao L, Zhang Y, Liu J, Yin W, Jin D, Wang D and Zhang W: miR-185 inhibits the proliferation and invasion of non-small cell lung cancer by targeting KLF7. Oncol Res 27: 1015-1023, 2019.
49. An YX, Shang YJ, Xu ZW, Zhang QC, Wang Z, Xuan WX and Zhang XJ: STAT3-induced long noncoding RNA LINC00668 promotes migration and invasion of non-small cell lung cancer via the miR-193a/KLF7 axis. Biomed Pharmacother 116: 109023, 2019.
50. Roberts JT and Borchert GM: Computational prediction of MicroRNA target genes, target prediction databases, and web resources. Methods Mol Biol 1617: 109-122, 2017.
51. Yang X, Li L, Huang Q, Xu W, Cai X, Zhang J, Yan W, Song D, Liu T, Zhou W, et al: Wnt signaling through snail1 and zeb1 regulates bone metastasis in lung cancer. Am J Cancer Res 5: 748-755, 2015.
52. Zhang L, Gallup M, Zlock L, Finkbeiner W and McNamara NA: P120-catenin modulates airway epithelial cell migration induced by cigarette smoke. Biochem Biophys Res Commun 417: 49-55, 2012.
53. Liu S, Ye D, Guo W, Yu W, He Y, Hu J, Wang Y, Zhang L, Liao Y, Song H, et al: G9a is essential for EMT-mediated metastasis and maintenance of cancer stem cell-like characters in head and neck squamous cell carcinoma. Oncotarget 6: 6887-6901, 2015.
54. Nilsen TW: Mechanisms of microRNA-mediated gene regulation in animal cells. Trends Genet 23: 243-249, 2007.
55. Cullen BR: Transcription and processing of human microRNA precursors. Mol Cell 16: 861-865, 2004.
56. Lu TX and Rothenberg ME: MicroRNA. J Allergy Clin Immunol 141: 1202-1207, 2018.
57. Yousef M Showe L and Showe M: A study of microRNAs in silico and in vivo: Bioinformatics approaches to microRNA discovery and target identification. Febs J 276: 2150-2156, 2009.
58. Cui J, Li D, Zhang W, Shen L and Xu X: Bioinformatics analyses combined microarray identify the deregulated microRNAs in oral cancer. Oncol Lett 8: 218-222, 2014.
59. Swamynathan SK: Krüppel-like factors: Three fingers in control. Hum Genomics 4: 263-270, 2010.
60. Dong JT and Chen C: Essential role of KLF5 transcription factor in cell proliferation and differentiation and its implications for human diseases. Cell Mol Life Sci 66: 2691-2706, 2009.
61. Sue N, Jack BH, Eaton SA, Pearson RC, Funnell AP, Turner J, Czolij R, Denyer G, Bao S, Navajas JC, et al: Targeted disruption of the basic Krüppel-like factor gene (Klf3) reveals a role in adipogenesis. Mol Cell Biol 28: 3967-3978, 2008.
62. Gray S, Wang B, Orihuela Y, Hong EG, Fisch S, Haldar S, Cline GW, Kim JK, Peroni OD, Kahn BB and Jain MK: Regulation of gluconeogenesis by krüppel-like factor 15. Cell Metab 5: 305-312, 2007.
63. Huo X, Li SW, Shi T, Suo A, Ruan Z, Guo H and Yao Y: Cullin3 promotes breast cancer cells metastasis and epithelial-mesenchymal transition by targeting BRMS1 for degradation. Oncotarget 6: 41959-41975, 2015.
64. Dellinger TH, Planutis K, Tewari KS and Holcombe RF: Role of canonical wnt signaling in endometrial carcinogenesis. Expert Rev Anticancer Ther 12: 51-62, 2012.
65. Anastas JN and Moon RT: WNT signalling pathways as therapeutic targets in cancer. Nat Rev Cancer 13: 11-26, 2013.
66. Choi YS, Shim YM, Kim SH, Son DS, Lee HS, Kim GY, Han J and Kim J: Prognostic significance of E-cadherin and beta-catenin in resected stage I non-small cell lung cancer. Eur J Cardiothorac Surg 24: 441-449, 2003.
67. Leung CO, Mak WN, Kai AK, Chan KS, Lee TK, Ng IO and Lo RC: Sox9 confers stemness properties in hepatocellular carcinoma through Frizzled-7 mediated Wnt/β-catenin signaling. Oncotarget 7: 29371-29386, 2016.
68. Mao Y, Xu J, Li Z, Zhang N, Yin H and Liu Z: The role of nuclear β-catenin accumulation in the twist2-induced ovarian cancer EMT. PLoS One 8: e78200, 2013.